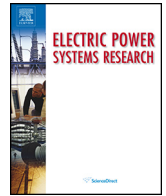




Contents lists available at [ScienceDirect](#)

Electric Power Systems Research

journal homepage: www.elsevier.com/locate/epsr



Variation of additional losses at no-load and full-load for a wide range of rated power induction motors

M. Dems^a, K. Komez a^{a,*}, J-Ph. Lecointe^b

^a Institute of Mechatronics and Information Systems, Lodz University of Technology, Stefanowskiego 18/22, 90-924 Lodz, Poland

^b Laboratoire Systèmes Electrotechniques et Environnement, Artois University, Technoparc Futura, Béthune 62400, France

ARTICLE INFO

Article history:

Received 11 August 2015
Received in revised form 8 July 2016
Accepted 17 October 2016
Available online xxx

Keywords:

Analytical modelling
Induction motors
Magnetic losses
Finite element method

ABSTRACT

This paper presents a comparison of losses at no load and full load of six different induction motors which rated powers are between 3 kW to 280 kW. The results show that additional core losses are strongly dependent on the load of the motor. The reason is the saturation of rotor tips which leads to an increase of the effective slot openings and the strengthening of harmonic by the induced currents in rotor cage. That leads to significant increase in additional core losses concomitant with motor load increases. For loss calculations, field-circuit and analytical methods are used. Using the FEM is presented an in-depth analysis of the phenomena at no-load and load indicating the reasons for increasing losses at the load conditions. Additionally, improved analytical method was employed to calculate the curves of stray losses versus load power. The results for no-load losses, stray losses and efficiency are compared with the measurements and good agreement was obtained for both field-circuit and analytical method. The change of stray losses versus output power was compared with formula proposed by IEC 60034-2-1 standard. The assigned values of stray load loss were found to be generally lower than average test result for motor with rated power below 18.5 kW and generally higher for motors with bigger rated power. In situations where a fixed value of stray load losses may be required the obtained curves can be used.

© 2016 Elsevier B.V. All rights reserved.

1. Introduction

The problem of electrical energy consumption has been the subject of several years of research in many international scientific centres. This problem has been particularly exacerbated in recent years, due to high energy intensity reduction requirements for various industrial systems [1]. In a wide range of high-power induction motors, the issue of energy consumption has been largely solved, especially since these motors have a relatively high efficiency. This increase is the result of fundamental and stray losses reduction due to technological improvements. It is possible to include them during the motor design stage, but this requires an improved accuracy in the calculation of the motor power losses.

The history of studying the phenomenon of additional (stray) losses in induction machines is very long. In Ref. [2] authors stated that this study start at the beginning of the previous century. Correct understanding of sources of those losses can be found in Ref. [3]. In Ref. [4] authors define components of stray load losses as: leakage

flux losses, high-frequency losses, pulsation losses, cross-current losses and surface losses.

The use of FEM time stepping analysis for computation of stray losses starting from the 90s and continues until today [5–13]. There were also the developments of classical analytical methods [14,15].

In numerous publications indicated a statement that for stray loss is responsible increase in the core loss under load [12,16]. Additionally, we can indicate that this phenomenon is also described as an interaction of so cold zig-zag flux introduced in classical theory of electrical machines. In Ref. [14] there were mentioned the load-dependent iron saturation of the tooth tips due to the air-gap zig-zag flux and corresponding tooth flux pulsation under load in the stator and rotor teeth. In Ref. [17] authors investigated the influence of the slot opening on losses but not enough attention has focused on saturation.

We agree that the stray loss are also affected by interbar current losses [4,9,18]. But in Ref. [19] initial idea of the authors was to prove that most of stray losses are losses due to inter-bar currents especially for the motor with skewed rotor bars. Surprisingly it turned out that the stray-load losses were 10% higher for the unskewed rotor, compared to the skewed rotor.

There is still a phenomena require further investigation e.g. the influence of the change in core temperature under load [20].

* Corresponding author. Fax: +48 426362309.

E-mail addresses: krzysztof.komez a@p.lodz.pl, krzysztof.komez a@gmail.com (K. Komez a).

<http://dx.doi.org/10.1016/j.epsr.2016.10.042>

0378-7796/© 2016 Elsevier B.V. All rights reserved.

Nomenclature

α	Exponent applied to the maximal value of the flux density for the eddy current losses
β	Exponent applied to the maximal value of the flux density for the hysteresis losses
B_m	Peak value of magnetic flux density
$B_p(n)$	Value of flux density component for sample number n .
B_{pk}	Complex value of magnetic flux density k th harmonic
f	Frequency
k	Harmonic order
k_e	Eddy current loss density coefficient
k_h	Hysteresis loss density coefficient
N	Number of sample points
ϑ	Position of the rotor in a given time instant
$\nu_{s(r)}$	Rank of the stator (rotor) harmonic component
w_{Fe}	Specific iron losses for frequency of the $\nu_{s(r)}$ stator (rotor) harmonic field and peak value of the stator (rotor) flux density due to the $\nu_{s(r)}$ harmonic
P_{in}	Input power of the motor
P_{out}	Output power of the motor
P_{ac}	Additional core losses for higher harmonics
P_{al}	Additional losses in the rotor cage, caused by current induced by field harmonics of the stator windings
P_{alb}	Additional losses from leakage flux of the connection leading of the stator windings
P_{ask}	Additional losses due to skew of rotor slots
P_a	Sum additional losses P_{al} , P_{alb} and P_{ask}
P_{SSL}	Stray losses

The problem of stray losses calculation is still topical. Stray losses are determined mainly by measurements according to the IEEE std 112 or IEC 60034-2-1 standards [21,22]. In our case all measurements were conducted according to the IEC 60034-2-1 standard using direct method. Stray losses are calculated from the power balance after deducting stator and rotor windings losses, friction and windage losses and core losses.

The aim of this paper is to evaluate additional core losses using a field-circuit method and all components of stray losses using analytical model [23–27]. Selecting the method of solution should be remembered about the uncertainty of parameters (up to a few percent) and the effects of various factors and phenomena on the losses [28–32]. The classical induction motor theory and its equivalent circuit show that the core losses caused by fundamental harmonic of magnetic flux density slightly decrease from no-load to rated load of the motor. But this theory does not take into account the fact that the additional losses in the core increase with the load and may even surpass the basic losses [33–37]. The stray losses increase in the motor core in comparison to no-load state (even if powered by AC voltage). It is caused by increases of the harmonic field amplitudes due to the influence of rotor currents as well as the saturation of the tooth heads caused by rotor leakage flux. This also causes secondary harmonics growth generated by rotor movement with effectively open rotor teeth.

2. Objects of investigation

Six different sized induction motors with cast aluminum slots and motor cores made from non-oriented silicon steel have been examined. The rated data of these motors are given in Table 1.

3. No-load and rated-load core losses

Calculations of no-load and full-load core losses were conducted using: an analytical approach implemented in the STAT.F algorithm, taking accounts the additional losses in the core due to the higher harmonics of the magnetic field, both in the stator and in the rotor and field-circuit numerical approach [23–27].

In all the calculations, the magnetic loss curves for a toroidal sample of non-oriented silicon steel M600-50A, M400-50A and M350-50A were measured as a function of the magnetic flux density and frequency up to 2000 Hz. These experimental results for non-oriented silicon steel M600-50A were given in Ref. [24]. They are shown for non-oriented silicon steel M400-50A and M350-50A in Fig. 1.

Calculations of losses have necessitated extrapolating the specific loss characteristic of the material for frequencies above 2000 Hz (Tables 2–4).

$$w_{Fe} = k_e f^2 B_m^\alpha + k_h f B_m^\beta \quad (1)$$

The proposed method of approximation is specifically aimed to find the solution for many harmonics. Many authors try to make an approximation of the surface losses or an approximation to a wider range of frequencies [38–49]. However, this leads to large errors which require changing coefficients as a complicated function (high order polynomials) of flux density and frequency. The method proposed by the authors provides better accuracy and is less complex than multi-variable polynomial response surface function (MVPRS) fitting approach presented in Ref. [50].

Calculations of losses using the field-circuit approach have been performed using the method described in detail in [27]. The field-circuit analysis is done for 2-D structure of the motors with frequency equal 50 Hz. For that purpose the Opera-2d/RM was chosen with the transient eddy current solver extended to include the effects of rigid body (rotating) motion and connection of external circuits. The machine was running at synchronous speed and feed with sinusoidal voltage. The time-stepping analysis was run over 10 periods of the supply voltage up the steady state was reached. After this time several snapshots are taken for next voltage period. Rotor cage, even rotating at synchronous speed, is subjected to the magnetic flux density change due to slotting. Therefore, additional losses occurrence can be notice. These losses are comparably high up to several percent of total losses. This part of losses is calculated as an average value taken from all time snapshots. A number of sample points were chosen to allow for the subsequent Discrete Fourier Transform (DFT) analysis. 200 points were in fact used. Using the values of x and y components of magnetic flux density in each element calculated at sample points, the DFT analysis was performed in order to assess the contribution of higher harmonics

$$B_{pk} = \sum_{n=0}^{N-1} B_p(n) e^{-i2\pi kn/N} \quad p = x \text{ and } y \quad k = 0, 1, \dots, \frac{N}{2} \quad (2)$$

The components of the flux density were calculated in the stationary frame of reference. The DFT applied to elements of the rotor moving with the rotor necessitate a simple transformation in terms of the rotor position angle.

$$\begin{aligned} B_{x(tf)} &= B_{x(sf)} \cos(\vartheta) + B_{y(sf)} \sin(\vartheta) \\ B_{y(tf)} &= -B_{x(sf)} \sin(\vartheta) + B_{y(sf)} \cos(\vartheta) \end{aligned} \quad (3)$$

The number of calculated harmonics was selected according to the Nyquist–Shannon sampling theorem as half of the number of sample points. The core losses in each element were evaluated using the specific core loss expression (1).

Using described 2D field-circuit method is only possible to determine the additional core losses and higher harmonics losses

متن کامل مقاله

دریافت فوری ←

ISIArticles

مرجع مقالات تخصصی ایران

- ✓ امکان دانلود نسخه تمام متن مقالات انگلیسی
- ✓ امکان دانلود نسخه ترجمه شده مقالات
- ✓ پذیرش سفارش ترجمه تخصصی
- ✓ امکان جستجو در آرشیو جامعی از صدها موضوع و هزاران مقاله
- ✓ امکان دانلود رایگان ۲ صفحه اول هر مقاله
- ✓ امکان پرداخت اینترنتی با کلیه کارت های عضو شتاب
- ✓ دانلود فوری مقاله پس از پرداخت آنلاین
- ✓ پشتیبانی کامل خرید با بهره مندی از سیستم هوشمند رهگیری سفارشات